Computer Networks 57 (2013) 3039–3050

Contents lists available at ScienceDirect

Computer Networks

journal homepage: www.elsevier.com/locate/comnet

Optimal adaptive channel scheduling for scalable video broadcasting over MIMO wireless networks

Chao Zhou, Xinggong Zhang, Zongming Guo *

Institute of Computer Science & Technology, Peking University, Beijing 100871, PR China

ARTICLE INFO

Article history:
Received 9 April 2012
Received in revised form 12 July 2013
Accepted 13 July 2013
Available online 25 July 2013

Keywords:
Adaptive channel scheduling
Scalable video broadcasting
Multi-input multi-output
Unequal error protection
Branch-and-bound algorithm

ABSTRACT

Video broadcasting is an efficient way to deliver video content to multiple receivers. However, due to heterogeneous channel conditions in MIMO wireless networks, it is challenging for video broadcasting to map scalable video layers to proper MIMO transmit antennas to minimize the average overall video transmission distortion. In this paper, we investigate the channel scheduling problem for broadcasting scalable video content over MIMO wireless networks. An adaptive channel scheduling based unequal error protection (UEP) video broadcasting scheme is proposed. In the scheme, video layers are protected unequally by being mapped to appropriate antennas, and the average overall distortion of all receivers is minimized. We formulate this scheme into a non-linear combinatorial optimization problem. It is not practical to solve the problem by an exhaustive search method with heavy computational complexity. Instead, an efficient branch-and-bound based channel scheduling algorithm, named TBCS, is developed. TBCS finds the global optimal solution with much lower complexity. The complexity is further reduced by relaxing the termination condition of TBCS, which produces a $(1-\varepsilon)$-optimal solution. Experimental results demonstrate both the effectiveness and efficiency of our proposed scheme and algorithm. As compared with some existing channel scheduling methods, TBCS improves the quality of video broadcasting across all receivers significantly.

1. Introduction

The broadcast nature of wireless medium allows a single source to simultaneously communicate information with multiple receivers. However, one major challenge for wireless broadcasting arises from heterogeneous network conditions of different receivers. Moreover, the potentially low bandwidth and high bit error rate also become significant obstacles for wireless communication providers to offer high quality multimedia services. To overcome such obstacles, multi-input multi-output (MIMO) systems, which have been investigated to simultaneously transmit multiple bit streams to achieve high data rate wireless multimedia communication [1], have emerged as one of the most prominent techniques. MIMO channel can be decomposed into a series of independent SISO subchannels [2], and it is suitable for transmitting multiple video substreams simultaneously. Meanwhile, the technology of scalable video coding (SVC) [3,4] enables media providers to generate a single embedded bitstream, from which appropriate subsets can be extracted to meet various requirements of a broad range of users. These conditions inspire us to combine the advanced MIMO and SVC techniques to improve the video broadcasting performance. SVC video consists of layers with different contribution to video quality, which makes it possible be transmitted with unequal error protection (UEP) [5–7]. In MIMO unicast, UEP can be easily achieved by mapping

* Corresponding author. Tel.: +86 10 82529726; fax: +86 10 82529207.
E-mail addresses: zhouchaoyf@pku.edu.cn (C. Zhou), zhangxg@pku.edu.cn (X. Zhang), guozongming@pku.edu.cn (Z. Guo).

1389-1286
http://dx.doi.org/10.1016/j.comnet.2013.07.010

video layers to antennas in the order of antenna's signal to noise ratio (SNR) strength [6]. However, it is not trivial for video broadcasting over MIMO wireless networks, and this has not drawn enough research attention.

Adaptive channel scheduling, which denotes mapping video layers to proper antennas to improve video transmission performance, faces great challenges for scalable video broadcasting over MIMO wireless networks. It mainly arises from that each transmit antenna corresponds to multiple receivers with different and independent SNR strength, and the corresponding SNR strength for each transmit antenna among multiple receivers forms a vector. For example, in Fig. 1, antenna A_{t1} is corresponding to three receivers ($A_{t1} - User1$, $A_{t1} - User2$, $A_{t1} - User3$), whose SNR strength form the vector $\Upsilon_1 = [\gamma_{11}, \gamma_{12}, \gamma_{13}]$. It is the same for antenna A_{t2}. since sets of vectors cannot be sorted, UEP cannot be achieved by mapping video layers to antennas in the order of antenna's SNR strength as done in MIMO unicast. Besides, the inter-layer dependencies among SVC video layers further make the problem challenging.

In this paper, we have studied this problem and proposed a novel adaptive channel scheduling based scalable video broadcasting scheme, which greatly improve the received video quality. By mapping each video layer to certain transmit antenna, the video layers are protected unequally and the overall average video quality is improved. Since each antenna faces multiple users with various network conditions as Fig. 1 shows, and there exists inter-layer dependencies among SVC video layers, the channel scheduling problem is a non-linear combinatorial problem. It can be solved using an exhaustive search method, which has the highest accuracy level and computational complexity. In order to reduce the complexity and make it suitable for practical implementation, a branch-and-bound framework is adopted to find an adaptive channel scheduling algorithm. Specifically, by partitioning the original problem into some simple subproblems, we are able to derive the upper and lower bounds of the average overall video distortion. Then an efficient branch-and-bound based channel scheduling algorithm (TBCS) is presented by incorporating these bounds into the branch-and-bound framework. With bounding and pruning techniques, TBCS finds the global optimal solution with much lower complexity than the exhaustive search method. Moreover, by relaxing termination conditions of TBCS, the complexity is further reduced and a $(1-\varepsilon)$-optimal solution is produced. Through simulations, TBCS is shown to be effective and efficient. As compared with existing channel scheduling schemes, the simulation results reveal significant performance improvements in TBCS.

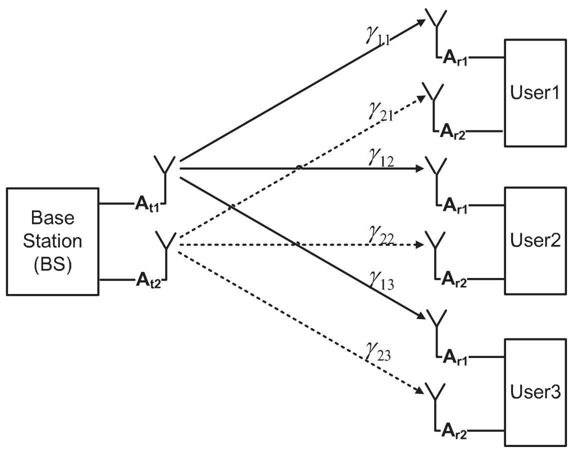

Fig. 1. Example of video broadcasting in MIMO wireless networks.

The main contributions of our work are summarized as:

- We are among the first to investigate the channel scheduling problem for salable video broadcasting over MIMO wireless networks where video layers are broadcasted to all users simultaneously over multiple antennas. Different from traditional multiuser problem over MIMO broadcast channel where different information is conveyed to different users by multiple transmit antennas, the antennas are shared by all users who receive all streams broadcasted over the antennas in our proposed scheme.
- We formulate it into a non-linear combinatorial optimization problem, and an efficient channel scheduling algorithm is proposed by employing the branch-and-bound framework. Specifically, by mapping the video layers to antennas according to the order of antennas' average PER, we derive the upper bound of the average overall video transmission distortion. On the other hand, we transform the channel scheduling problem to an assignment problem by relaxing some constraints, and then the lower bound of the average overall video transmission distortion is derived.
- By relaxing the termination condition of TBCS, a $(1-\varepsilon)$-optimal solution is produced to balance the needs for the complexity and accuracy of the proposed algorithm.

This paper is organized as follows. We review related work in Section 2. In Section 3, we describe our proposed system and formulate the proposed scheme into a non-linear combinatorial optimization problem. In Section 4, we propose a branch-and-bound framework to solve the channel scheduling problem. First, we derive the upper bound (Section 4.2) and and lower bound (Section 4.3) of the average overall distortion respectively, then an efficient branch-and-bound based channel scheduling algorithm is proposed, which produces the global optimal solution (Section 4.4). Also, an acceleration mechanism is presented to further reduce the computational complexity (Section 4.5). We show simulation results in Section 5, and conclude the paper in Section 6.

2. Related work

In recent years, MIMO systems have emerged as one of the most prominent techniques [1,8–10] to provide high data rate wireless communications. Spatial multiplexing techniques [1,10] have been investigated to simultaneously transmit independent data in order to achieve high data rate wireless multimedia communications. For MIMO broadcast, the capacity region is still an open issue since broadcast channels are non-degraded generally. But the optimal sum rate, and the suggestive pre-coding scheme are now completely known. Caire and Shamai [11] are the first to give the optimal sum capacity of MIMO broadcast channel by explicitly maximizing the Dirty Paper [12] lower bound and minimizing the Sato's upper bound [13] in the case which, as it turns out, is equal. But its computational complexity is high and it is hard to be extended to more general cases [14]. Yang [15] extends the channel scheduling scheme from unicast MIMO network to multicast MIMO network. In [16], dynamic resource allocation is studied to maximize system's capacity, and a low complexity suboptimal algorithm is proposed for practical implementation. Literature [17] investigates multi-resolution broadcast systems for WCDMA cellular mobile networks, including MIMO technology. However, all of these previous works focus on maximizing system's capacity and belong to parallel transmission (PT) [18] MIMO. In PT MIMO, all the content is treated equally and it is not suitable for video communication, since video content generally contains bits with different importance, and needs to be protected unequally when transmitted over error-prone wireless networks. In unicast, UEP in MIMO can be easily achieved by mapping video layers to multiple transmit antennas in the order of antenna's signal to noise ratio (SNR) strength [6]. While in MIMO broadcast networks, it becomes challenging. This is mainly because that each transmit antenna corresponds to multiple end users, and the SNR strength of each transmit antenna forms a vector as Fig. 1 shows.

The idea of scalable video for multiuser communications is well-known. Without loss of generality, multiuser MIMO is used to convey different information to different users by multiple transmit antennas. In [19], the authors propose a video broadcasting scheme via pre-coding and SNR-Scalable video coding. By packet extraction and pre-coding, users will receive different quality of videos. There are some other research works on multiuser MIMO [20–22]. However, we differ from them in several major ways. For the purpose of clarity, we take [19] as example to compare our proposed scheme with these works. First, by the pre-coding matrix which is consist of some orthogonal sub-matrices, the antennas are divided into some independent groups and each user will only receive the stream transmitted by a certain group of antennas in [19]. In our proposed scheme, each user will receive the streams transmitted over all antennas. Therefore, this kind of multiuser video transmission schemes have great limitation in the number of users that the number of transmit antennas is no smaller than the sum of all users receive antennas as assumed in [19]. We have no such limitation on both the number of users and number of antennas since all users multiplex the same transmit antennas. At last, in [19], some streams are transmitted multiple times at the transmitter side which wastes bandwidth and power resource, for example, the base layer must transmitted in each group of antennas for each user. While in our proposed scheme, each video layer is only mapped to a certain antenna and broadcasted to all users.

Very few UEP schemes have been proposed for broadcasting scalable video over MIMO wireless networks where multiple antennas have been sufficiently multiplexed for broadcasting multiple streams to all users concurrently. In [23], UEP is achieved by using diversity embedded space time codes (DESTC), which provides UEP to different video layers, thereby delivering high quality video to users with good network conditions while still providing acceptable quality to users with poor network conditions. But the authors assume that all receivers employ single receive antenna, which greatly simplifies the problem. Moreover, DESTC is not flexible enough to adapt to the complex network environment because it add different amount of redundancy to different streams without considering the instantaneous channel conditions. A novel JSCC framework for scalable video transmission has been proposed in [24], in which power allocation, channel coding and modulation are jointly optimized to achieve UEP and improve the system performance. The computational complexity is very high and it is not suitable for practical implementation. In [25], UEP is achieved for scalable video broadcasting over cooperative wireless networks through power allocation. However, all of these previous works treat transmit antennas equally and neglect their various qualities. In fact, the qualities of transmit antennas are time-varying, and video transmission performance can be greatly improved by mapping video layers to antennas properly.

To the best of our knowledge, none of previous research work considers achieving UEP for scalable MIMO video broadcasting through channel scheduling. In this paper, we investigate this problem, and an adaptive channel scheduling based video broadcasting scheme is proposed. We formulate this scheme into a non-linear combinatorial problem. By adopting the branch-and-bound framework, an effective and efficient low-complexity channel scheduling algorithm is proposed.

3. Problem formulation

In this section, the proposed system architecture is described at first. Then we formulate the adaptive channel scheduling based scalable video broadcasting scheme into a non-linear combinatorial optimization problem.

3.1. System description

Fig. 2 shows the block diagram of our proposed system, where all transmitter and receivers are equipped with multiple antennas. Here we only show one receiver for the purpose of clarity, and all receivers have the same signal processing diagrams. At the transmitter side, the input video sequence is encoded to generate multiple video layers by H.264/SVC [3,4]. Combining with the feedback

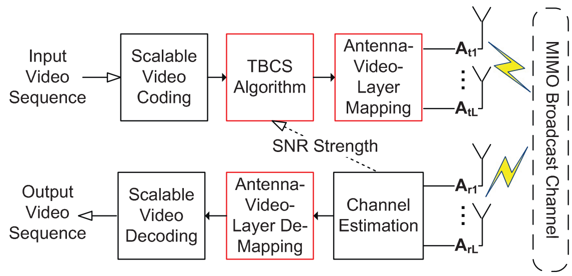

Fig. 2. Proposed system diagram.

SNR strength and video layers' unequal importance, the video layers are periodically switched among multiple transmit antennas using our proposed TBCS algorithm. Then the video layers are broadcasted to all receivers simultaneously. At the receiver side, each receiver needs to estimate the post-processing SNR strength of each transmit antenna and send it back to the transmitter by employing pilot symbols [26]. The transmitted video sequences are reconstructed after demodulation and channel decoding.

Without loss of generality, it is commonly assumed that the channel is block fading [27], i.e., the channel remains constant over some consecutive symbol periods (determined by the coherence time) and then changes in an independent fashion to a new realization. The above video broadcasting system can be treated as K virtual MIMO unicast systems except that all receivers have the same transmitter, and K is the total number of receivers [28]. Then, for each virtual MIMO system with M_t transmit antennas and M_r receive antennas over flat-fading channel, the system equation between the transmitter and kth receiver is

$$\mathbf{y}_k = \sqrt{\frac{E_s}{M_t}}\mathbf{H}_k\mathbf{x} + \zeta_k \tag{1}$$

where $\mathbf{H}_k$ is the complex channel matrix between the transmitter and kth receiver with size $M_r \times M_t$,$\mathbf{x}$ is the $M_t \times 1$ transmitted signal vector, $\mathbf{y}_k$ is the $M_r \times 1$ received signal vector at kth receiver, ζ_k is the $M_r \times 1$ noise vector with elements distributed according to $\mathcal{CN}(0, N_0)$, and E_s is the total average energy available at the transmitter over a symbol period having removed losses due to propagation and shadowing.

The channel matrix $\mathbf{H}_k$ is estimated by existing estimation methods such as maximum-likelihood (ML) and minimum mean-squared error (MMSE) techniques discussed in [26] at kth ($1 \leqslant k \leqslant K$) receiver. More details of channel estimation can also refer to literature [6]. The transmitted signals are detected by linear ZF (zero-forcing) receivers, which are much more practically attractive than non-linear receivers due to their low complexity. Then, the post-processing SNR strength of ith transmit antenna for kth receiver, γ_{ik}, is obtained as

$$\gamma_{ik} = \frac{E_s}{M_t N_0 \left[\mathbf{H}_k^{\mathrm{H}}\mathbf{H}_k\right]_{ii}^{-1}} \tag{2}$$

where $[\cdot]_{ii}$ denotes ith diagonal entry of the matrix inside the square bracket, and $\mathbf{H}^{\mathrm{H}}$ denotes the Hermitian of $\mathbf{H}$.

In this work, we focus on exploiting the potential UEP ability of channel scheduling for scalable video broadcasting over MIMO system. To eliminate the effect of channel coding and modulation, which can also achieve UEP, we fix the modulation level and channel coding rate for all video layers. In fact, our proposed channel scheduling method can be incorporated with these methods to further improve the system performance, one of the incorporation examples is our previous JSCC work [29]. Specifically, M-QAM and RS (N,m) are used for modulation and channel coding, where N is block size, and m is the number of source bits in each block. Then, combining with the feedback SNR strength in Eq. (2), we can easily derive the block error rate $b_{ik}(i \leqslant M_t, k \leqslant K)$ between transmit antenna i and receiver k as follows:

$$b_{ik} = 1 - \sum_{j=0}^{N-m}\binom{N}{j}\rho_{ik}^{j}(1-\rho_{ik})^{(N-j)} \tag{3}$$

where $\rho_{ik} \approx \frac{\sqrt{M-1}}{\sqrt{M}\log_2\sqrt{M}}\mathrm{erfc}\left(\sqrt{\frac{3\gamma_{ik}}{2(M-1)}}\right)$ is the bit error rate (BER) between ith transmit antenna and kth receiver, and erfc $(\cdot)$ is the complementary error function.

3.2. Problem formulation

Suppose the transmitter is equipped with M_t antennas, user k is equipped with M_r^k antennas, and the video sequence is encoded into L layers. Generally, each video layer is broadcasted over one transmit antenna or dropped at the transmitter side due to the data-rate constraints. We define $\mathbf{A}_{L\times M_t} = \{a_{ij}\}$ as channel scheduling matrix to denote the mapping relationship between video layers and transmit antennas, and its entries $a_{ij} \in \{0,1\}$. Let $a_{ij} = 1$ if ith video layer is transmitted over jth transmit antenna, or $a_{ij} = 0$ otherwise. Then, we have

$$\sum_{j=1}^{M_t} a_{ij} \leqslant 1 \tag{4}$$

when $\sum_{j=1}^{M_t} a_{ij} = 1$, it denotes video layer i is mapped to one of the antennas, and $\sum_{j=1}^{M_t} a_{ij} = 0$ denotes video layer i is mapped to no antenna and dropped at the transmitter side. Then, we derive the video layer's PER matrix $\mathbf{P}_{L\times K} = \{P_{jk}\}$ as a function of matrix $\mathbf{A}_{L\times M_t}$ as follows:

$$P_{ik} = \begin{cases} \sum_{j=1}^{M_t}(a_{ij}b_{jk}) & \text{if } \sum_{j=1}^{M_t} a_{ij} = 1 \\ 1 & \text{if } \sum_{j=1}^{M_t} a_{ij} = 0 \end{cases} \tag{5}$$

where P_{ik} denotes the ith video layer's PER for user k, b_{ik} is the block error rate between ith transmit antenna and receiver k and it is given in Eq. (3).

We employed the quality model proposed in [30] to estimate the end-to-end video transmission distortion in our work. According to [30], the video quality (PSNR) after decoding all the first n layers is given as

$$\tilde{d}_n(q_n) = d_n(\tilde{m}, q_n) = b_1\log_{10}\left((\tilde{m}_n)^s + 1\right)\cdot q_n + b_2 \tag{6}$$

where b_1 and b_2 are model parameters, the value of s depends on the frame type, and q_n is the value of quantization parameter (QP) for layer n. More details about this can refer to literature [30] and the references therein. Then, the weight of each video layer is written as:

$$w_i = \begin{cases} \tilde{d}_1(q_1) & \text{if } i = 1 \\ \tilde{d}_i(q_i) - \tilde{d}_{i-1}(q_{i-1}) & \text{if } i \geqslant 2 \end{cases} \tag{7}$$

For the purpose of clarity, we omit the subscript of matrixes $\mathbf{A}$ and $\mathbf{P}$ in the following of the paper. Now, we get the end-to-end video transmission distortion $\mathcal{D}_k(\mathbf{P}(\mathbf{A}))$ for user k:

$$\mathcal{D}_k(\mathbf{P}(\mathbf{A})) = \sum_{i=1}^{L} w_i\left(1 - \prod_{j=1}^{i}(1 - P_{jk})\right) \tag{8}$$

and the overall average distortion for all users is:

$$D(\mathbf{P}(\mathbf{A})) = \frac{1}{K}\sum_{k=1}^{K}\mathcal{D}_k(\mathbf{P}(\mathbf{A})) \tag{9}$$

Moreover, we can also get the video bit-rate for each video layer according to literature [30] and we denote r_i as the video bit-rate of layer i. Under the assumption that RS (N, m) is used for channel coding, video layer i would consume the data-rate of r'_i for transmission with

$$r'_i = r_i \frac{N}{m} \tag{10}$$

We assume the data-rate capacity of antennas i is R_i. Since a fixed modulation order on all antennas is used, we have $R_1 = R_2 = \cdots = R_{M_t} = R$. Then, the proposed adaptive channel scheduling based video broadcasting scheme is formulated as:

$$\begin{aligned} \{\mathbf{A}^*\} = \arg\min\nolimits_{\{\mathbf{A}\}} \quad & D(\mathbf{P}(\mathbf{A})) \\ \text{subject to} \quad & \sum_{i=1}^{L} r'_i a_{ij} \leqslant R, \quad \forall j \leqslant M_t \\ & \sum_{j=1}^{M_t} a_{ij} \leqslant 1, \quad \forall i \leqslant L \\ & a_{ij} = \{0, 1\}, \quad \forall i \leqslant L,\ j \leqslant M_t \end{aligned} \tag{11}$$

The above optimization problem aims to minimize the average overall video transmission distortion through adaptive channel scheduling, i.e., selecting the optimal matrix $\mathbf{A}^*$. However, due to the heterogeneous network conditions of different receivers and inter-layer dependencies among SVC video layers, solving this problem is challenging. Exhaustive search method finds the optimal solution by searching the whole solution space, whose size is M_t^L. Its computational complexity increases heavily with the number of transmit antennas and video layers, and it is not suitable for practical implementation.

4. Branch-and-bound based adaptive channel scheduling

In this section, we adopt the branch-and-bound framework to solve above channel scheduling problem, and an efficient branch-and-bound based channel scheduling algorithm is proposed. We first briefly describe how to adopt the branch-and-bound framework into channel scheduling. Then, the upper and lower bounds of the average overall distortion for each subproblem are derived in detail. At last, we present TBCS to solve the optimization problem in Eq. (11).

4.1. Branch-and-bound based channel scheduling

Branch-and-bound is an iterative method for solving optimization problems, especially for discrete and combinatorial problems. A branch-and-bound procedure has two components. The first one, which is called *branching*, is to partition a problem into subproblems. The procedure is repeated recursively to each of the subproblems and all produced subproblems naturally form a tree structure, i.e., the *branch-and-bound tree*. Its nodes are the constructed subproblems. The leaves of the tree are also call the *Problem List*. The other component is *bounding*, which is a fast way of finding upper and lower bounds for the optimal solution for each subproblem.

The core of this approach is an observation that, for a minimization problem, if the lower bound for a subproblem s_2 is higher than the upper bound for any other subproblem s_1, s_2 and the branch rooted at s_2 can be safely discarded from the tree, thus the computational complexity can be reduced. This procedure is called *pruning*. Besides, for each iterative, the subproblem with the smallest lower bound is selected and further partitioned. The algorithm terminates when the lower bound is equal to the upper bound.

In our proposed adaptive channel scheduling based video broadcasting scheme, we partition the problem into subproblems by selecting available transmit antennas for the video layers orderly, i.e., we first select a transmit antenna for the base layer, then for the first enhancement layer, and so on. When computing the upper and lower bounds of the average distortion for the nodes in the dth layer of the *branch-and-bound tree*, we only need to compute the bounds for the remaining $L - d$ video layers. This is because all the first d video layers have been mapped to certain antennas, and their corresponding distortion is determined.

In order to reduce the iterations, *pruning* procedure is used to discard nodes from the tree. The key of *pruning* is to obtain the bounds for each node. For our proposed minimization problem, any feasible solution can be treated as the upper bound. On the other hand, an lower bound is found by solving a relaxed problem. The details of deriving these bounds are presented in Section 4.2 and Section 4.3 respectively.

Before presenting how to derive the upper and lower bounds, we present Proposition 1 as follows, which servers as an intuition to develop the distortion bounds.

Proposition 1. *In unicast, when the scalable video layers are mapped to multiple transmit antennas according to the order of PER (the base layer is transmitted over the antenna with the smallest PER, the first enhancement layer is transmitted over the antenna with the second smallest PER, and so on), the minimum video transmission distortion is obtained.*

The proof is given in Appendix A. □

4.2. Upper bound

The objective of above optimization problem is to minimize the average overall video transmission distortion by selecting the optimal channel scheduling matrix $\mathbf{A}^*$. For this proposed minimization problem, any matrix that satisfies the constraints described in Eq. (11) is a feasible solution, and its corresponding average overall distortion is an upper bound. Though it is very easy to find such matrixes, it is not trivial to find an appropriate matrix which obtains a tight upper bound. This is very crucial for reducing the number of iterations.

In Proposition 1, we show that the optimal matrix $\mathbf{A}^*$ can be easily obtained according to the order of antenna's PER in MIMO unicast. The proposition also denotes that the principle of channel scheduling is to map important video layers to antennas with better channel quality (low PER). MIMO broadcast channel is a vector channel, i.e., each transmit antenna corresponds to multiple receivers, and the corresponding PER forms a vector. Since sets of vectors cannot be sorted, it is hard to determine which antenna has the best or worst channel quality. In order to find a feasible solution providing a tight upper bound, average PER of each transmit antenna is adopted to denote its channel quality in TBCS. Then, the channel scheduling problem is similar to that in unicast. It is worth to noticing that more than one video layers may be mapped to the same antenna when the data-rate constraints are satisfied, thus we cannot simply map the video layers to transmit antennas in the order of their average PER according to Proposition 1. However, the intuition of mapping video layers to antennas behind Proposition 1 is that from the lowest layer to the highest layer, we map video layer i to antenna j when it has lowest average PER and its *remaining available data-rate* is no smaller than the required rate r_i'. Then, the *remaining available data-rate* of antenna j is updated by subtracting r_i'. This process is iterated until all video layers have been mapped to appropriate antennas or there is no antennas whose *remaining available data-rate* satisfies the data-rate constraints. Though the solution is not optimal, its performance is much better than random channel scheduling, and a much tighter upper bound is obtained.

We denotes P_i^{avg} as the average PER of ith antenna, then we have

$$P_i^{avg} = \frac{1}{K}\sum_{k=1}^{K} b_{ik} \tag{12}$$

For nodes in dth layer of the *branch-and-bound tree*, each of the first $d(1 \leqslant d \leqslant L)$ video layers has been mapped to a certain transmit antenna respectively. This denotes that the values $a_{ij}(1 \leqslant i \leqslant d, 1 \leqslant j \leqslant M_t)$ have been determined as described in Section 4.1. Then for $\forall d < i \leqslant L$, $1 \leqslant j \leqslant M_t$, the value of a_{ij} is derived as follows:

$$a_{ij} = \begin{cases} 1, & \text{if } P_j^{avg} = \min(\Psi_i) \\ 0, & \text{otherwise} \end{cases} \tag{13}$$

where Ψ_i is the set of antenna's average PER, excluding the antennas whose *remaining available data − rate* is no smaller than r_i'. Until now, we have obtained the values for all entries in matrix $\mathbf{A}$. According to formula Eqs. (2)–(9), the upper bound $\mathcal{D}^{upper}$ of the average overall distortion can be easily derived.

4.3. Lower bound

In order to obtain the lower bound of average overall distortion, we first define an efficiency matrix $\mathbf{V} = \{v_{ij}\}$ to denote video layers' distortion, and its entry v_{ij} denotes ith video layer's average distortion among all users when it is mapped to jth transmit antenna. The entries are dependent due to the inter-dependence among video layers. We derive approximate expression of lower bounds for the entries in $\mathbf{V}$, which have eliminated the dependence among them. Then, the primal problem is transformed into a standard assignment problem (AP), and the optimal solution (minimal total average distortion) of this AP is the primal problem's lower bound.

Now, we give details of deriving the lower bound of average overall distortion. For the nodes in dth layer of the *branch-and-bound tree*, the values $a_{ij}(1 \leqslant i \leqslant d, 1 \leqslant j \leqslant M_t)$ have been determined as described in the above section. Then we can easily derive $P_{ik}(1 \leqslant i \leqslant d, 1 \leqslant k \leqslant K)$ according to Eq. (5). Now the average overall distortion of the first d video layers is

$$\mathcal{D}^d = \frac{1}{K}\sum_{k=1}^{K}\sum_{i=1}^{d} w_i \left(1 - \prod_{j=1}^{i}(1 - P_{jk})\right) \tag{14}$$

Therefore, in order to obtain the lower bound of the average overall distortion, we only need to derive the lower bound of average distortion for the remaining $L - d$ video layers. According to the inter-dependence among video layers, v_{ij} is written as

$$v_{ij} = \frac{1}{K}\sum_{k=1}^{K} w_i \left(1 - \prod_{s=1}^{i}(1 - P_{sk})\right), \quad \forall d+1 \leqslant i \leqslant L \tag{15}$$

where for user k $(1 \leqslant k \leqslant K)$, $P_{ik} = b_{jk}$ since ith video layer is mapped to jth antenna, and $P_{sk}(1 \leqslant s \leqslant d)$ are constant as explained in the second paragraph of this sub-section. Therefore, v_{ij} is only depending on $P_{sk}(d+1 \leqslant s \leqslant i-1)$. Now we can write Eq. (15) as

$$\begin{aligned} v_{ij} &= \frac{1}{K}\sum_{k=1}^{K} w_i \left(1 - \prod_{s=1}^{d}(1 - P_{sk}) \prod_{s=d+1}^{i-1}(1 - P_{sk})(1 - P_{ik})\right) \\ &\leqslant \frac{1}{K}\sum_{k=1}^{K} w_i \left(1 - \prod_{s=1}^{d}(1 - P_{sk}) \prod_{s=d+1}^{i-1}(1 - \min(\Psi_{s,j}^k))(1 - b_{jk})\right) \\ &= v_{ij}' \end{aligned} \tag{16}$$

where $\Psi_{s,j}^k$ is the set of antenna's PER for user k, excluding those whose *remaining available data-rate* is no smaller than r_i'. When a layer is mapped to a certain antenna, its *remaining available data-rate* is updated by the video layer's bit-rate including redundancy bit-rate. The intuition of this inequality comes from Proposition 1, and it is derived by selecting the feasible antenna with smallest PER for sth $(d+1 \leqslant s \leqslant i-1)$ video layer iteratively. Moreover, for any video layer i, when there is no antenna whose *remaining available data-rate* is no smaller than r_i', or $\Psi_{s,j}^k$ is a null set, it denotes video layer i must be dropped at the transmitter side. In this case, we simply set $v_{ij}' = w_i$.

Since v_{ij}' is a lower bound of v_{ij} and it is independent from each other, the efficiency matrix $\mathbf{V}'$ for the assignment problem is written as:

$$\mathbf{V}' = \begin{pmatrix} v_{(d+1)1}' & \cdots & v_{(d+1)(L-d)}' \\ \vdots & \ddots & \vdots \\ v_{L1}' & \cdots & v_{L(L-d)}' \end{pmatrix} \tag{17}$$

This assignment problem can be solved by any existing algorithms, such as dynamic programming or recursive iteration algorithms. Its optimal solution, denoted as $\mathcal{D}^{(L-d)}$, is the lower bound of the remaining $L - d$ video layers' total distortion for the primal problem. Then, we derive the lower bound of the average overall distortion of all video layers as

$$\mathcal{D}^{lower} = \mathcal{D}^{d} + \mathcal{D}^{(L-d)} \tag{18}$$

4.4. Adaptive channel scheduling algorithm

We incorporate these bounds into the branch-and-bound framework, and an efficient branch-and-bound based channel scheduling algorithm is proposed. Compared with exhaustive search method, TBCS finds the global optimal solution with much lower complexity.

Fig. 3 illustrates the convergence of TBCS as d increase. For a certain selected *node* in the *branch-and-bound tree*, d denotes both its layer-index in the *tree* and the number of video layers that have been assigned antennas for this *node*. The figure shows that when $d = L$, i.e., the selected *node* is a *leaf* in the *branch-and-bound tree*, the upper bound is equal to the lower bound and the algorithm terminates. The pseudo code for the branch-and-bound based channel scheduling algorithm is given in Algorithm 1. The algorithm consists of three major components: (i) Partition component partitions the primal problem into subproblems, (ii) Bounding component derives the upper and lower bounds of each subproblem, (iii) Iteration and Pruning component compares the bounds and delete some subproblems to reduce the complexity.

Moreover, we accelerate the convergence of TBCS and further reduce the complexity by relaxing its termination condition. The algorithm terminates when the upper bound reaches $1 + \varepsilon$ of the lower bound, i.e., $UB - LB = LB * \varepsilon$, and a $(1 - \varepsilon)$-optimal solution is produced. The details of this acceleration mechanism are presented in Section 4.5.

4.5. Enhancement

Instead of terminating the algorithm when the bounds are equal, we introduce a $(1 - \varepsilon)$-optimal solution method to accelerate the convergence of TBCS, i.e., TBCS terminates when the upper bound reaches $1 + \varepsilon$ of the lower bound. Let the global optimal objective value be $G \leqslant UB$, we have

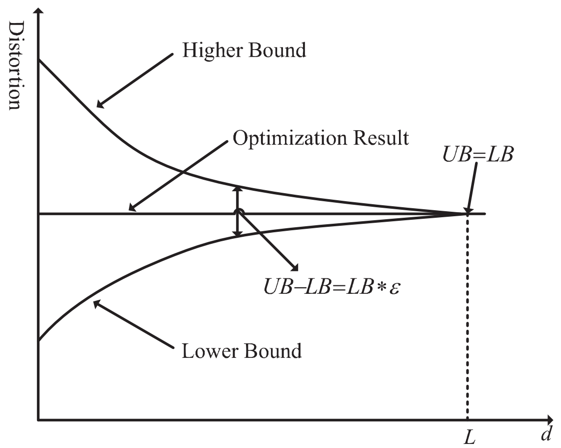

Fig. 3. Convergence of TBCS as d increases, and d denotes the number of video layers that have been mapped to certain antennas.

$LB \geqslant \frac{1}{1+\varepsilon} UB \geqslant \frac{1}{1+\varepsilon} G = (1 - \varepsilon + \varepsilon^2 - \varepsilon^3 + \cdots) \approx (1 - \varepsilon)G$, for $0 \leqslant \varepsilon \ll 1$. By relaxing the termination condition, we greatly speed up the convergence of the branch-and-bound algorithm.

Algorithm 1. Branch-and-bound based channel scheduling algorithm

---

Initialization:

1: obtain the original problem as Prob 1;
2: optimal solution $sol \leftarrow \emptyset$;
3: problem list $\mathcal{S} \leftarrow \{\text{Prob } 1\}$;
4: upper bound $UB \leftarrow \infty$;
5: lower bound $LB \leftarrow 0$;
6: feasible antenna set $\mathcal{A} \leftarrow \{1, 2, \ldots, M_t\}$;
7: layer-index for the selected *node* in the *branch-and-bound tree* $d_1 \leftarrow 0$;
8: get the upper bound UB_1 and solution $\mathbf{A}_1$ as described in Section 4.2;
9: get the lower bound LB_1 as described in Section 4.3;
10: $UB \leftarrow UB_1$;
11: $LB \leftarrow LB_1$;

Iteration and Pruning:

1: select Prob l with the smallest LB_l in $\mathcal{S}$;
2: $LB \leftarrow LB_l$;
3: **if** $UB_l < UB$ **then**
4: $sol \leftarrow \mathbf{A}_l$;
5: $UB \leftarrow UB_l$;
6: **end if**
7: **if** $UB \leqslant (1 + \varepsilon)LB$ **then**
8: stop with solution sol;
9: **else**
10: remove all Prob k in $\mathcal{S}$ with $LB_k \geqslant \frac{UB}{1+\varepsilon}$;
11: **end if**

Partition:

1: for the selected Prob l;
2: **while** $\mathcal{A} \neq \emptyset$ **do**
3; select antenna m in $\mathcal{A}$, and map the $(d_l + 1)$th video layer to antenna m;
4: update $\mathcal{A}$
5: $d_{l_m} \leftarrow d_l + 1$
6: obtain a new problem Prob l_m;
7: **end while**

Bounding:

1: solve all the partition Probs l_m to get solution $\mathbf{A}_{l_m}$ and bounds UB_{l_m} and LB_{l_m};
2: remove Prob l from problem list $\mathcal{S}$;
3: **for** each m **do**
4: **if** $LB_{lm} \leqslant \frac{UB}{1+\varepsilon}$ **then**
5: add Prob l_m into problem list $\mathcal{S}$;
6: **end if**
7: **end for**
8: **if** $\mathcal{S} == \emptyset$ **then**
9: stop;
10: **else**
11: goto the *Iteration* & *Pruning* procedure;
12: **end if**

---

5. Illustrative simulation results

In this section, we present illustrative simulation results to show how the proposed channel scheduling scheme is able to achieve UEP, and how TBCS finds the global solution with much lower complexity than exhaustive search method. In order to evaluate both the effectiveness and efficiency of our proposed scheme and algorithm, we have compared them with exhaustive search method, which always achieves the optimum with the highest computation complexity. Besides, we have also compared them with Min–Max channel scheduling scheme (which selects antennas in the ascending order of the maximal PER of each row in matrix $B_{L\times K}$, and the inspiration comes from [31]) and random channel scheduling method (RCS, which randomly assigns a transmit antenna for each video layer and it is similar to PT MIMO [18]). The video sequences, *mobile*, *foreman* and *crew*, are tested. These sequences are selected because of their different characteristic motion and spatial details. All test sequences are 300 frames with a frame rate of 30 fps and encoded by the JSVM reference encoder [4] to generate an embedded scalable video stream with eight layers.

We assume that the channel conditions of the users are independent. For user k ($1 \leqslant k \leqslant K$), the MIMO channel is under independent Rayleigh fading, and elements in channel matrix $\mathbf{H}_k$ are obtained from Clarke and Jakes' model [32]. Noise vector ζ_k is from i.i.d. Gaussian collection with zero mean, independent real and imaginary parts, with variance σ^2. Equal power is allocated to each transmit antenna and 16-QAM is used for modulation. Also, RS codes [33] are adopted to protect the transmitted bit streams since it maintains maximum erasure protection while produces a minimum of redundancy. We allocate the same channel codes for all video layers. Although unequal power allocation and channel coding can also achieve UEP, these methods are beyond the scope of this paper. In this paper, we focus on achieving UEP only through channel scheduling and it can be easily incorporated into these existing UEP schemes. For the detection of transmitted video signals, linear ZF receivers [34] are adopted.

5.1. Complexity analysis

We conduct experiments to show the computational complexity of TBCS *versus* exhaustive search method. The number of *iterations* is adopted as the comparison criterion. Fig. 4 illustrates the *iterations* of both exhaustive search method and TBCS under different number of video layers with the number of transmit antennas $M_t = 4$. The figure shows that exhaustive search method always has higher iterations than TBCS. In order to find the global optimal solution, exhaustive search method has to search the whole solution space, whose space size is M_t^L. While the computational complexity of TBCS is mainly depending on the tightness of both the upper and lower bounds, branching and pruning techniques, and parameter ε. Their effectiveness is demonstrated through simulation results in the next subsections. In the case that $\varepsilon = 0$, TBCS finds the optimal solution, but it has much lower complexity than exhaustive search method, this also demonstrates the efficiency of TBCS.

From this figure, we also find that the iterations gap between exhaustive search method and TBCS is becoming bigger as L increases. This is mainly because that in exhaustive search method, the number of iterations is only depending on the number of video layers when M_t is constant, and it is increasing exponentially. While in TBCS, the video layers have been mapped to antennas orderly. Thus, when some important video layers (base layer and some relative low enhancement layers) are mapped to antennas with very poor channel quality, many *nodes* would be pruned from the *branch and bound tree* through the *pruning* procedure. This greatly reduces the searching space and computational complexity.

5.2. BER performance

We then compare both the short-term and long-term average BER of different schemes. The number of transmit antennas is four and the number of video layers is eight in the simulations. Elements in channel matrix $\mathbf{H}_k$ are obtained from Clarke and Jakes' model [32]. For purpose of clarity, the parameter ε is set to zero in TBCS, and we only plot the average BER of four layers (the lowest two layers and the highest two layers, i.e., the base layer, enhance-1, enhance-6 and enhance-7) of different schemes in this subsection.

The short-term average BER of video layers with average $SNR = 20$ dB is illustrated in Fig. 5. The figures clearly demonstrate that the short-term average BER is timely fluctuated from 10^{-6} to 10^{0}. Thus, video layers should be mapped to different transmit antennas according to their importance. Specially, in order to protect base-layer bit stream during bad status, mapping it to the best antenna is indispensable. In RCS scheme, all video layers are treated equally and mapped to transmit antennas randomly. The average BER of all video layers are fluctuated from 10^{-6} to 10^{0} as Fig. 5(a) shows, and UEP is not achieved. The Min–Max scheme assigns the antennas to video layers in the ascending order of the maximal PER of each row in matrix $\mathbf{B}_{L\times K}$ [31], and the average BER of video layers is illustrated in Fig. 5(b). The figure shows that the average BER still does not strictly have the same order with that of video layers' priorities. However, when compared with

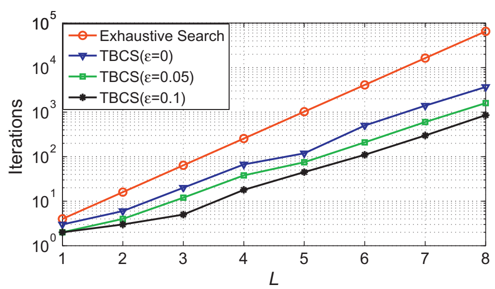

Fig. 4. Complexity performance. The iterations of exhaustive search method and TBCS with different ε *versus* the number of video layers L. The number of antennas $M_t = 4$, the number of users $K = 50$, average $SNR = 20$ dB.

RCS, important video layers are given more protection in some degree. For example, the average BER of the lowest two layers is generally lower than the highest two layers. Our proposed branch-and-bound algorithm finds the optimal video-layer-antenna mapping order and Fig. 5(c) shows its average BER results of different video layers. This figure obviously manifests that an unequal average BER according to the importance of bit stream is accomplished. However, at some points, such as when $t = 0.2$ and $t = 0.9$, the average BER of lower video layers is not always lower than that of higher layers. This is because channel scheduling is a non-linear mapping problem due to the interdependence among video layers, and simply mapping video layers to multiple antennas according to the order of average BER is only a feasible solution. Though it cannot guarantee the solution's optimality, it generally achieves much better performance than RCS. This is why we adopt the average PER as the criterion to denote antenna's channel quality and find an upper bound of the average overall distortion in TBCS, the details have been explained in Section 4.2.

We also compare the long-term average BER of each video layer under different SNR strength and the results are illustrated in Fig. 6. In RCS scheme, the long-term average BER will be converged since all the video layers are treated equally and mapped to multiple transmit antennas randomly. Fig. 6(a) demonstrates this. The figure shows that all video layers nearly have the same average BER, and no UEP is achieved. On the other hand, the long-term average BER performance illustrated in Fig. 6(b) shows that low video layers have lower average BER than the high layers in Min–Max scheme. However, the gap of the average BER among video layers is small. It is mainly because that Min–Max only gives more protection to important video layers in some degree, and it cannot guarantee that optimal UEP is achieved. In Fig. 6(c), we plot the long-term average BER of TBCS. The figure clearly shows that UEP is achieved, and the gap of the average BER among video layers is bigger than that in Min–Max scheme. When comparing all the three sub-figures in Fig. 6, we can find that the low average BER of the important video layers (e.g. base layer, the first enhancement layer) is achieved by sacrificing the BER performance of high video layers. This is reasonable in video communication since video signal contains bits of different importance. And it is indispensable to protect the bits discriminatively and give more protection to the important bits.

5.3. Reconstructed video PSNR performance

We conduct experiments to show the reconstructed average overall PSNR of the decoded video sequences over various average SNR strength and number of receivers. Three video sequences, *mobile*, *foreman* and *crew*, are tested and encoded into eight layers.

First, we evaluate the reconstructed average PSNR performance over various SNR strength and the results are illustrated in Fig. 7. The number of receivers $K = 50$ and parameter $\varepsilon = 0$. All the three figures, Fig. 7(a–c), undoubtedly show that the PSNR improvement is achieved by TBCS against both RCS and Min–Max schemes. The performance improvement is from the obtained UEP, which is achieved by adaptive channel scheduling. Particularly, the gap of PSNR among the schemes in the low SNR region is outstanding since the high BER makes it indispensable to give more protection to the important video layers. As the average SNR strength increases, the superiority of channel scheduling becomes inconspicuous. Suppose that SNR strength of any antenna is high enough to broadcast video layer reliably, channel scheduling is becoming unnecessary. Therefore, the gap of PSNR among the schemes is very small in the high SNR region.

We also compare the schemes under different numbers of receiver, and the results are illustrated in Fig. 8. The average SNR strength is 20 dB and parameter $\varepsilon = 0$. From the figures we find that PSNR is decreasing as the number of users K increases. The reason is that the heterogeneity of channel condition is becoming considerable as the number of users increases, and the performances of all schemes are deteriorated. When the number of users K is large enough, the quality differentiation among antennas is becoming inconspicuous since each antenna is corresponding to K subchannels, and the gap of PSNR among the schemes becomes small. Meanwhile, the figures also clearly show that TBCS always performs the best, this demonstrates the effectiveness of TBCS under various channel conditions.

We then examine the influence of parameter ε on received video quality. The video sequence, *crew*, is tested, and the number of users $K = 50$. Fig. 10 plots the average PSNR of the reconstructed video given different ε. The figure shows that average PSNR decreases as ε increases. The reason is as follows. When $\varepsilon = 0$, TBCS finds the optimal solution and has the same PSNR performance with exhaustive search method. When $\varepsilon > 0$, TBCS terminates when $LB \geqslant \frac{1}{1+\varepsilon} UB$ as described in Section 4.5, and a $(1-\varepsilon)$-opti-

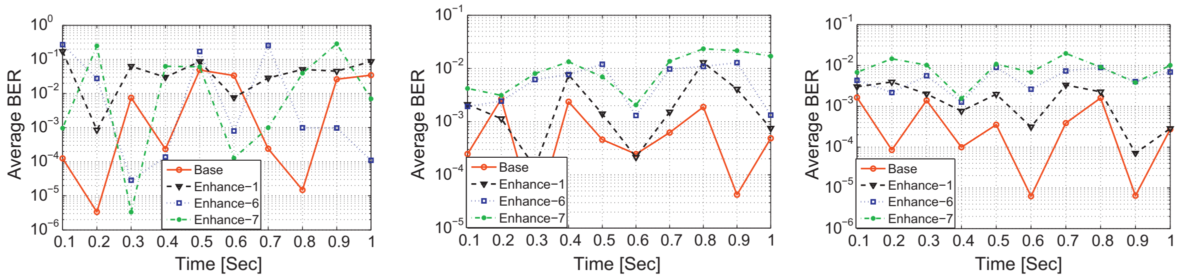

(a) RCS. (b) Min-Max. (c) TBCS.

Fig. 5. Short-term average BER of different schemes. The number of users $K = 50$, average $SNR = 20$ dB, and $\varepsilon = 0$.

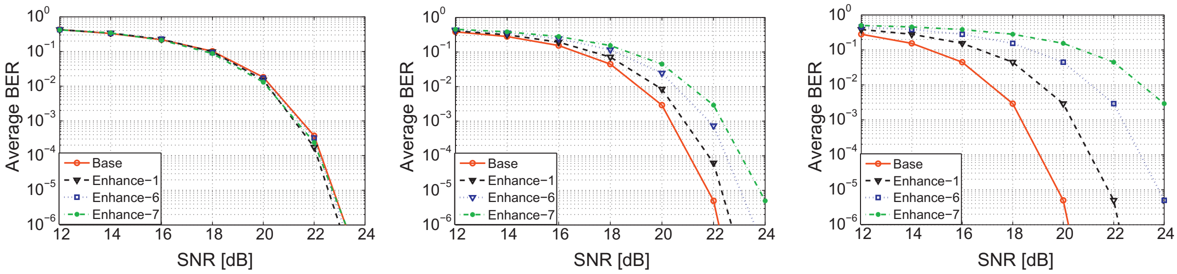

(a) RCS. (b) Min-Max. (c) TBCS.

Fig. 6. Long-term average BER of different schemes. The number of users $K = 50$, and $\varepsilon = 0$.

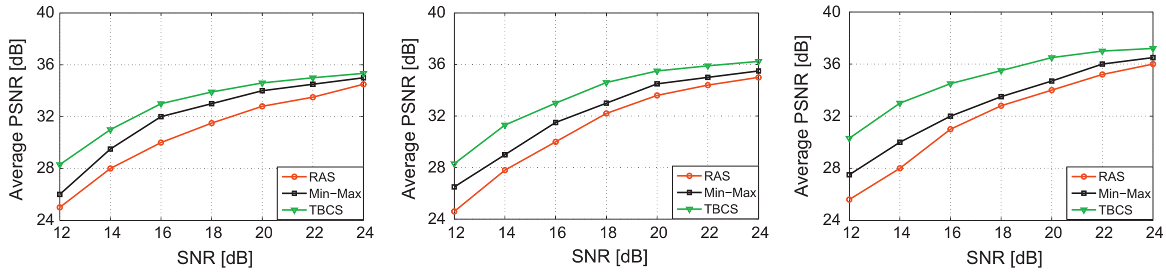

(a) Reconstructed average PSNR of *mobile*. (b) Reconstructed average PSNR of *foreman*. (c) Reconstructed average PSNR of *crew*.

Fig. 7. The reconstructed average PSNR performance of different schemes under various SNR strength. The number of users $K = 50$, and $\varepsilon = 0$.

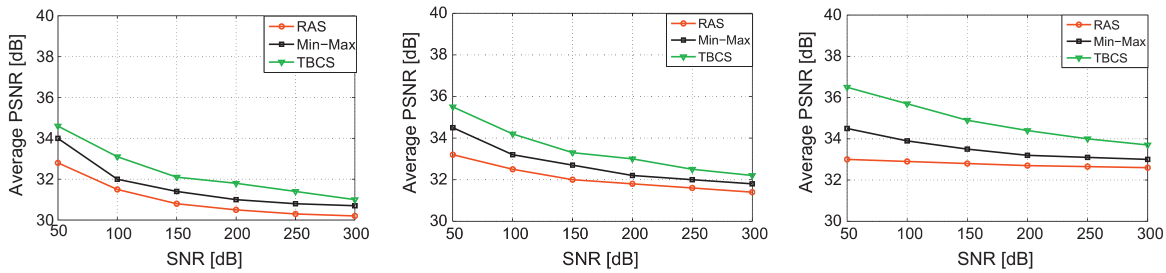

(a) Reconstructed average PSNR of *mobile*. (b) Reconstructed average PSNR of *foreman*. (c) Reconstructed average PSNR of *crew*.

Fig. 8. The reconstructed average PSNR performance of different schemes under various number of users. Average $SNR = 20$ dB, and $\varepsilon = 0$.

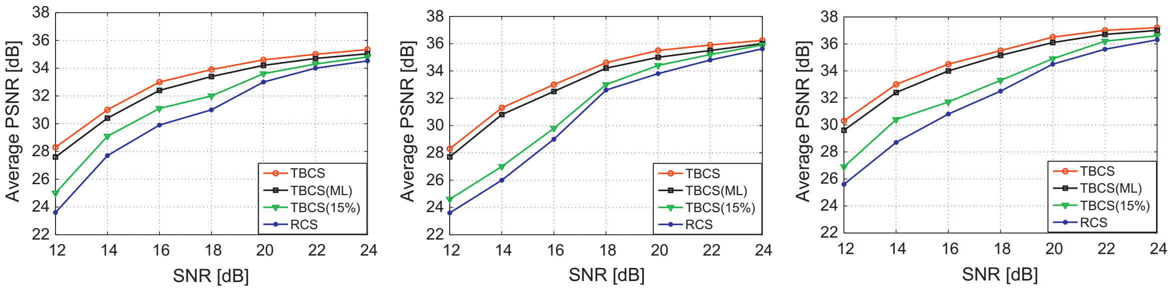

(a) Reconstructed average PSNR of *mobile*. (b) Reconstructed average PSNR of *foreman*. (c) Reconstructed average PSNR of *crew*.

Fig. 9. The reconstructed average PSNR performance against channel estimation error. The number of users $K = 50$.

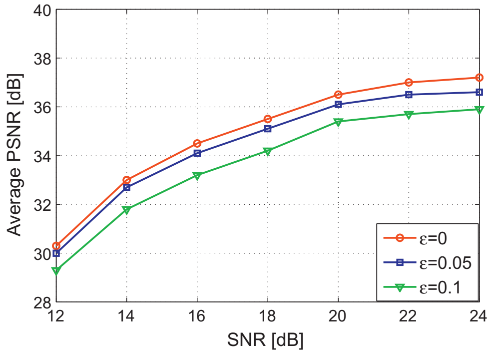

Fig. 10. The influence of parameter ε on average PSNR performance. The number of users $K = 50$.

mal solution is produced, which is equal to the upper bound of the distortion. As ε increases, the algorithm converges more quickly with higher distortion. From Fig. 4 and Fig. 10, we can also conclude that TBCS is flexible to various applications. For example, if the applications require high video quality, the parameter ε should be set small. On the other hand, if the applications require low delay, ε can be set big relatively.

At last, we investigate the reconstructed video PSNR performance of TBCS against the channel estimation error. In Fig. 9, we show the results with perfect channel matrix $\mathbf{H}_k$ *versus* channel estimation error where H_k is estimated by ML. Moreover, to investigate the robustness of TBCS under heavy estimation error, we also plot results when we add 15% disturbances to the feedback SNR strength. Specifically, from the channel matrix, we get the SNR strength of each antenna according to Eq. (2). Then, each of the SNR strength γ_{ik} is disturbed by randomly adding a noise, and the noise is a variable randomly selected from the range of $[-0.15 * \gamma_{ik}, 0.15 * \gamma_{ik}]$. At last, the performance of RCS is illustrated as the benchmark. The figures show that when channel matrix is estimated by ML, the PSNR performance is very close to the case when channel matrix is known perfectly. This demonstrates the effectiveness of our proposed scheme and algorithm in practical applications. When the estimation error is heavy which is simulated by adding 15% disturbances to the feedback SNR strength in our experiments, the PSNR is close to RCS, but it is never worse than RCS. This is because when the estimation error is too big, it provides little useful information for optimizing channel scheduling and the channel scheduling result is similar to RCS. This demonstrates the robustness against channel estimation error.

6. Conclusion

In this paper, we have investigated the channel scheduling problem for scalable video broadcasting over MIMO wireless networks. According to the feedback SNR strength, the scalable video layers are periodically scheduled among multiple antennas. We formulate it into a non-linear combinatorial optimization problem. The computational complexity is very high by using exhaustive search method. Instead, by adopting the branch-and-bound framework, an efficient low-complexity channel scheduling algorithm is proposed. Moreover, at the expense of performance loss, the complexity is further reduced by relaxing termination condition of TBCS, and a $(1-\varepsilon)$-optimal solution is produced. Our proposed scheme is very flexible that UEP is achieved only by switching the video layers among multiple antennas. It can be easily incorporated into most of the existing UEP video transmission schemes. At last, simulation results demonstrate both the effectiveness and efficiency of our proposed scheme and algorithm.

Acknowledgments

This work was supported by National High-tech Technology R&D Program (863 Program) of China under Grant 2013AA013504, National Natural Science Foundation of China under contract No. 61071082 and National Key Technology R&D Program of China under Grant 2012BAH18B03.

Appendix A

Proof. In unicast, assuming that there are L video layers and L transmit antennas, we then denote P_i as the PER of ith transmit antenna, and assume that the PERs satisfy $P_1 < P_2 \cdots < P_L$. We also define $\mathcal{G} = [\mathcal{G}[1], \mathcal{G}[2], \ldots, \mathcal{G}[L]]$ as the video-layer-antenna mapping order, which denotes that ith video layer is mapped to $\mathcal{G}[i]$th antenna. According to Proposition 1, when $\mathcal{G}[i] = i(\forall 1 \leqslant i \leqslant L)$, the minimum video transmission distortion can be obtained:

$$\mathcal{D}^* = \sum_{i=1}^{L} w_i * \left(1 - \prod_{s=1}^{i}(1-P_s)\right) \tag{A.1}$$

We prove Proposition 1 through proof by contradiction. Assume that there exists another mapping order $\mathcal{G}' = [\mathcal{G}'[1], \mathcal{G}'[2], \ldots, \mathcal{G}'[L]]$, whose corresponding distortion, $\mathcal{D}'$, is smaller than D^*, i.e., $\mathcal{G}'[i] \neq i$ & $\mathcal{D}' < \mathcal{D}^*$, $\exists 1 \leqslant i \leqslant L$. Then the distortion $\mathcal{D}'$ is written as:

$$\mathcal{D}' = \sum_{i=1}^{L} w_i * \left(1 - \prod_{s=1}^{i}(1-P_{\mathcal{G}'[s]})\right) \tag{A.2}$$

Then

$$\Delta\mathcal{D} = \mathcal{D}^* - \mathcal{D}' = \prod_{s=1}^{i}(1-P_{\mathcal{G}'[s]}) - \prod_{s=1}^{i}(1-P_s) \leqslant 0 \tag{A.3}$$

Above inequality comes from that in $\prod_{s=1}^{i}(1-P_s)$, $P_s(\forall 1 \leqslant s \leqslant i)$ is sth smallest PER of all transmit antennas, so $\prod_{s=1}^{i}(1-P_s)$ is always no smaller than $\prod_{s=1}^{i}(1-P_{\mathcal{G}'[s]})$. Then we derive that $\Delta\mathcal{D} \leqslant 0$, i.e., $\mathcal{D}^* \leqslant \mathcal{D}'$.

Moreover, if and only if

$$\prod_{s=1}^{i}(1-P_{\mathcal{G}'[s]}) = \prod_{s=1}^{i}(1-P_s), \quad \forall 1 \leqslant i \leqslant L \tag{A.4}$$

the inequality takes the equal sign, i.e., $\mathcal{D}' = \mathcal{D}^*$, and $\mathcal{G}'[i] = i,\ \forall 1 \leqslant i \leqslant L$. This is contradictory with the assumption that $\mathcal{G}'[i] \neq i\ \&\ \mathcal{D}' < \mathcal{D}^*,\ \exists 1 \leqslant i \leqslant L$. Therefore, we conclude Proposition 1 is correct. □

References

[1] P.W. Wolniansky, G.J. Foschini, G.D. Golden, R.A. Valenzuela, V-BLAST: an architecture for realizing very high data rates over the rich-scattering wireless channel, in: IEEE Int. Symp. on Signals, Syst. Electron., 1998, pp. 295–300.

[2] D. Gesbert, M. Shafi, D. shan Shiu, P. Smith, A. Naguib, From theory to practice: an overview of MIMO space-time coded wireless systems, IEEE J. Sel. Areas Commun. 21 (3) (2003) 281–302.

[3] T. Wiegand, G. Sullivan, J. Reichel, H. Schwarz, M. Wien, Joint Draft of SVC Amendment, Joint Video Team (JVT), Doc. JVT-W201.

[4] H. Schwarz, D. Marpe, T. Wiegand, Overview of the scalable video coding extension of the H.264/AVC standard, IEEE Trans. Circ. Syst. Video Technol. 17 (9) (2007) 1103–1120.

[5] M.K. Jubran, M. Bansal, L.P. Kondi, Low-delay low-complexity bandwidth-constrained wireless video transmission using SVC over MIMO systems, IEEE Trans. Multimedia 10 (8) (2008) 1698–1707.

[6] D. Song, C.W. Chen, Scalable H.264/AVC video transmission over MIMO wireless systems with adaptive channel selection based on partial channel information, IEEE Trans. Circ. Syst. Video Technol. 17 (9) (2007) 1218–1226.

[7] Y.P. Fallah, H. Mansour, S. Khan, P. Nasiopoulos, H.M. Alnuweiri, A link adaptation scheme for efficient transmission of H.264 scalable video over multirate WLANs, IEEE Trans. Circ. Syst. Video Technol. 18 (7) (2008) 875–887.

[8] S.M. Alamouti, A simple transmit diversity technique for wireless communications, IEEE J. Sel. Areas Commun. 16 (8) (1998) 1451–1458.

[9] V. Tarokh, H. Jafarkhani, A.R. Calderbank, Space-time block coding for wireless communications: performance results, IEEE J. Sel. Areas Commun. 17 (3) (1999) 451–460.

[10] G.J. Foschini, Layered space-time architecture for wireless communication in a fading environment when using multi-element antennas, Bell Labs Tech. J. (1996) 41–59.

[11] G. Caire, S. Shamai, On the achievable throughput of a multiantenna Gaussian broadcast channel, IEEE Trans. Inf. Theory 49 (7) (2003) 1691–1706.

[12] M. Costa, Writing on dirty paper, IEEE Trans. Inform. Theory 29 (1983) 439–441.

[13] H. Sato, An outer bound on the capacity region of broadcast channel, IEEE Trans. Inform. Theory 24 (1978) 374–377.

[14] S. Vishwanath, N. Jindal, A. Goldsmith, On the capacity of multiple input multiple output broadcast channels, IEEE Int. Conf. Commun. 3 (2002) 1444–1450.

[15] Y. Yang, On the capacity of maximum selection in MIMO multicast network, IEEE Conf. on Comput. Commun. (2008) 1–5.

[16] J. Xu, S.-J. Lee, W.-S. Kang, J.-S. Seo, Adaptive resource allocation for MIMO-OFDM based wireless multicast systems, IEEE Trans. Broadcast. 56 (1) (2010) 98–102.

[17] A.M.C. Correia, J.C.M. Silva, Nuno M. B Souto, et al., Multi-resolution broadcast/multicast systems for MBMS, IEEE Trans. Broadcast. 53 (1) (2007) 224–234.

[18] H. Zheng, K.J.R. Liu, Space-time diversity for multimedia delivery over wireless channels, IEEE Int. Symp. Circ. Syst. 4 (2000) 285–288.

[19] J. Xu, R. Hormis, X. Wang, MIMO video broadcast via transmit-precoding and SNR-scalable video coding, IEEE J. Sel. Areas Commun. 28 (6) (2010) 456–466.

[20] G. Caire, S. Shamai, On the achievable throughput of a multi-antenna Gaussian broadcast channel, IEEE Trans. Inf. Theory 49 (7) (2003) 1691–1706.

[21] J. Xu, R. Hormis, X. Wang, Scalable video multicast on broadcast channels, IEEE Global Telecommun. Conf. (2009) 1–8.

[22] Y. Yang, On the capacity of maximum selection in MIMO multicast network, IEEE Conf. Comput. Commun. (2008) 1–5.

[23] C. Bilen, E. Erkip, Y. Wang, Layered video multicast using diversity embedded space time codes, IEEE Int. Symp. Sarnoff (2009) 1–5.

[24] H. Xiao, Q. Dai, X. Ji, W. Zhu, A novel JSCC framework with diversity-multiplexing-coding gain tradeoff for scalable video transmission over cooperative MIMO, IEEE Trans. Circ. Syst. Video Technol. 20 (7) (2010) 994–1006.

[25] C.-H. Kuo, C.-M. Wang, J.-L. Lin, Cooperative wireless broadcast for scalable video coding, IEEE Trans. Circ. Syst. Video Technol. 21 (6) (2011) 816–824.

[26] B. Hassibi, B. Hochwald, How much training is needed in multiple-antenna wireless links?, IEEE Trans Inf. Theory 49 (4) (2003) 951–963.

[27] E. Biglieri, J. Proakis, S. Shamai, Fading channels: information-theoretic and communications aspects, IEEE Trans. Inform. Theory 44 (6) (1998) 2619–2692.

[28] E. Biglieri, R. Calderbank, A. Constantinides, A. Goldsmith, A. Paulraj, H.V. Poor, MIMO Wireless Communications, Cambridge Univ. Press, Cambridge, UK, 2007.

[29] C. Zhou, X. Zhang, Z. Guo, A novel JSCC scheme for scalable video transmission over MIMO systems, IEEE Int. Image Process. (2012) 2277–2280.

[30] H. Mansour, Y. Fallah, P. Nasiopoulos, V. Krishnamurthy, Dynamic resource allocation for MGS H.264/AVC video transmission over link-adaptive networks, IEEE Trans. Multimedia 11 (8) (2009) 1478–1491.

[31] D. Lu, D.K.C. So, Performance based receive antenna selection for V-BLAST systems, IEEE Trans. Wireless Commun. 8 (1) (2009) 214–225.

[32] R.H. Clarke, A statistical theory of mobile-radio reception, Bell Syst. Tech. J. 47 (1968) 957–1000.

[33] S. Lin, D.J. Costello, Error Control Coding-Fundamentals and Applications, Prentice-Hall, Englewood Cliffs, NJ, 1983.

[34] A. Paulraj, R. Nabar, D. Gore, Introduction to Space-Timewireless Communications, Cambridge Univ. Press, Cambridge, UK, 2003.

Chao Zhou received the Bachelor's degree from Institute of Electronic Information & Control Engineering, Beijing University of Technology, Beijing, China, in 2009. He is currently a Ph.D. student in Peking University, Beijing, China. His current research interests include Error Protection for Video Communications, MIMO Communications and Wireless Streaming.

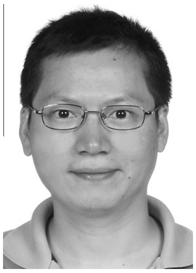

Xinggong Zhang received the Ph.D degree in computer science from Peking University, Beijing, China, in 2011. He is currently an Associate Professor at Peking University, Beijing, China. His current research interests include video communication, multimedia networking and optimization.

Zongming Guo received the Ph.D degree from Department of Computer Science, Peking University, Beijing, China, in 1994. He is now a professor of Institute of Computer Science & Technology, Peking University. His current research interests include video code/decode, scalable video code, video communication, image processing.